

Glass formation and crystallization in the $\text{GeSe}_2\text{-Sb}_2\text{Te}_3$ system

S. SURIÑACH, M. D. BARO, M. T. CLAVAGUERA-MORA
*Termologia, Facultad de Ciencias, Universidad Autónoma de Barcelona,
 Bellaterra (Barcelona), Spain*

N. CLAVAGUERA
*Física del Estado Sólido, Facultad de Física, Universidad de Barcelona, Diagonal, 645
 Barcelona-28, Spain*

The glass formation and crystallization of liquid-quenched $(\text{GeSe}_2)_{100-y}(\text{Sb}_2\text{Te}_3)_y$ alloys was investigated by means of differential scanning calorimetry, X-ray diffraction and optical and scanning electron microscopy. By water quenching glasses are obtained from compositions in the range $5 \lesssim y \lesssim 30$. Qualitative parametrization of glass-forming tendency gives, as best glass formers, alloys with $y \cong 20$. Crystallization on heating proceeds in one stage for glasses with $y \lesssim 20$ and in two stages for those with greater Sb_2Te_3 content. For compositions lying in the GeSe_2 primary crystallization region crystals appear preferentially at the surface of the sample, but for the other compositions ($24 \lesssim y \lesssim 30$) the crystals emerge in the bulk and often develop in spherulitic or axialitic form.

1. Introduction

For simple substances or congruently melting compounds there is a unique temperature for the equilibrium between liquid and crystal called the melting temperature, T_m . For a non-stoichiometric solution there is a solidification interval $\Delta T_s = T_l - T_s$, where T_l and T_s are respectively the liquidus and solidus temperatures. It is well known that the formation of a glass requires rapid cooling through ΔT_s in order to avoid the crystallization process. This procedure gives glasses with a frozen-in supercooled liquid structure, deep eutectic compositions being usually the best glass-formers. As there is no absolute criterion for glass formation, empirical parameters are extensively used for quantitative characterization. Some parameters are fundamentally kinetic, as for instance the change in free energy in the crystallization of the bulk liquid (homogeneous nucleation) introduced by Turnbull [1] and subsequently developed by Uhlmann [2, 3]. Structural parameters deal with atomic geometrical arrangement, bonding and atomic size effects. The more recent development

is due to Phillips [4-6]. Thermodynamic criteria were related to the heat of formation by Kolomiets [7] and more recently to the excessive melting point depression by Chen [8].

A qualitative description of glass-forming ability can be easily obtained from the thermal events observed on heating the glass by differential scanning calorimetry (DSC). The relevant structural transformations are the glass transition at T_g , shown in the DSC curve as a discontinuous increase of heat capacity, and the crystallization, with onset at T_x , which may have one or several exothermic peaks. Further heating results in the melting of the sample.

Since the crystallization of a chalcogenide glass is a highly exothermic process, DSC is a very suitable technique for obtaining both the effective activation energy for crystallization and the heat of crystallization. Of the rate equations commonly used in the kinetic analysis of reactions in condensed phases, the one which gives, in general, the best fit to the experimental values is the Johnson-Mehl-Avrami-Erofe'ev equation. Its application

in non-isothermal measurements has been extensively discussed. See for instance, Sestak [9] and Henderson [10]. One of its major advantages is the ease with which the activation energy can be evaluated by use of the so-called "peak" method. This method was first outlined by Kissinger [11, 12] for Eyring n th-order transformations, and is applicable to any transformation of very general form as explained by Henderson [10]. However the knowledge of the effective activation energy is insufficient for the proper interpretation of the crystallization process. Three distinct types of crystallization may occur: (a) polymorphic crystallization; (b) eutectic crystallization; and (c) primary crystallization of one of the phases. All these reactions can be understood at least qualitatively by using a hypothetical diagram of free energy against concentration for the different phases as exemplarized by Koster [13, 14]. The determination of crystalline species and morphologies involves X-ray diffraction and microscopy. The identification of nucleation and growth processes may be achieved by a combination of the above-mentioned techniques and DSC.

In this paper the results on the formation, thermal stability and crystallization of $(\text{GeSe}_2)_{100-y}(\text{Sb}_2\text{Te}_3)_y$ glasses prepared by quenching of the melt are presented and discussed. Previous studies [15] have shown that this system is quasi-binary. The phase diagram shows a limited solubility of GeSe_2 in Sb_2Te_3 , the solid solution limit being 43 mol% Sb_2Te_3 at the eutectic temperature 758 K. The eutectic is located at 24 mol% Sb_2Te_3 . It appears that in a substantial portion of the equilibrium diagram glasses are easy to obtain from quenching of the melt. The temperatures of the structural transformations characteristic of the glassy state and the effective activation energies of crystallization have been derived from DSC results. The morphology of the crystallization reaction has been investigated using optical and scanning electron microscopy. The transformation properties of the glasses as a function of the composition and their relation to the equilibrium diagram are discussed.

2. Experimental results

Quenched samples were prepared by melting weighed amounts of the elements (5N purity) in evacuated and sealed quartz ampoules. The molten alloys were held at 1275 K for 12 h and constantly agitated to ensure homogeneity; subsequently they

were quenched in water at room temperature. The glassy state of the samples was checked by X-ray powder diffraction.

Differential scanning calorimetry was carried out on about 10 mg of powdered material in a Perkin Elmer DSC 2 under pure argon atmosphere. Constant heating rate experiments were recorded, from room temperature to beyond the crystallization exotherms, at scan rates β ranging from 2.5 to 80 K min^{-1} . For morphological studies, some specimens were isothermally annealed for varying times in the DSC under argon. Specimens were also examined that had been continuously heated at 20 K min^{-1} to a specific point in the DSC curve and then quickly removed from the calorimeter and quenched to room temperature.

Microscopic observations were made to elucidate the origin of the heat effects observed in the DSC traces. Metallographic examination on mechanical polished samples was performed using a Leitz Ortholux II Pol BK optical microscope. Scanning electron microscope observations of fresh fracture surfaces were made by either an ISI S-III A SEM or a Phillips 500 SEM with an energy-dispersive spectrometer. X-ray diffraction was carried out on a Guinier de Wolf camera with $\text{CuK}\alpha$ radiation.

3. Results

3.1. Glass formation

Water quenching 0.5 g samples of molten alloy inside quartz ampoules of 5 mm internal diameter and 1 mm thickness, produces a cooling rate at the eutectic temperature of the order of 10^3 K min^{-1} . Depending on the composition, this method of preparation gives three types of specimens: (i) glassy, (ii) partially crystalline and (iii) crystalline samples. The DSC curves of the glassy samples show the glass transition and one or two crystallization peaks, depending on the composition, prior to the melting transformations. In the partially crystalline samples the heat evolved in the crystallization is much lower than that of melting, and no clear glass transition can be detected. The crystalline samples show only the melting transformations.

The temperature T_g of the glass transition and the temperatures $T_{p1}(T_{p2})$ of the peak of the first (second) crystallization exotherms are plotted, superimposed on the phase diagram, in Fig. 1. All glasses show a single glass transition, T_g , decreasing approximately at the same rate as T_1 with increasing Sb_2Te_3 content. Samples with

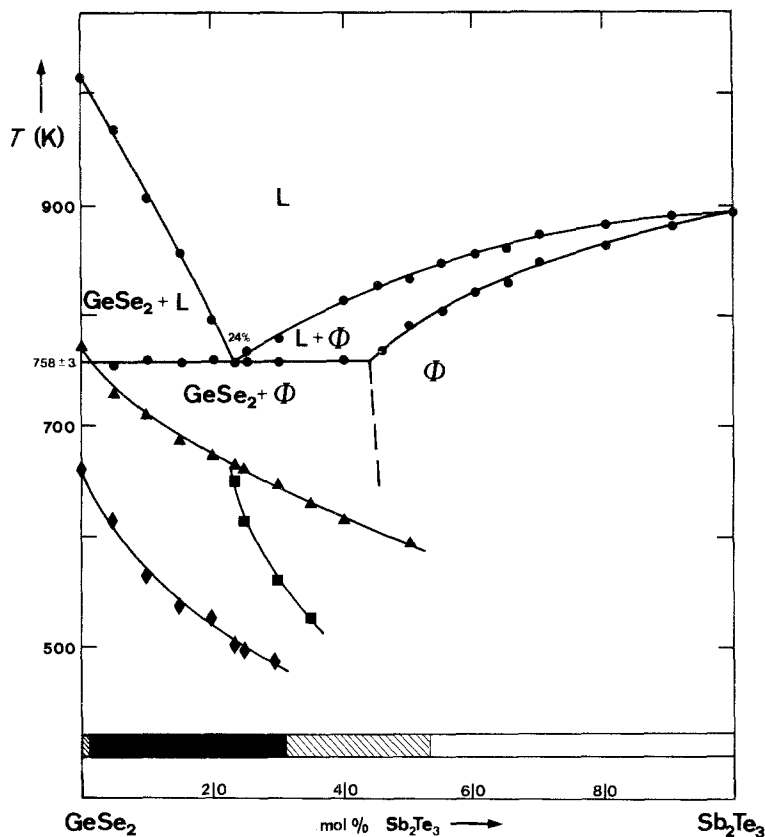


Figure 1 Glass-forming region, temperatures of the relevant structural transformations and phase diagram of the GeSe_2 - Sb_2Te_3 quasi-binary system. ■ glassy, ▣ partially crystalline and □ crystalline alloys. Temperatures of: (♦) glass transition, (■, ▲) peaks of crystallization, (●) solidus and liquidus. Heating rate: 20 K min^{-1} .

$y < 24$ show a single crystallization peak, but for a higher Sb_2Te_3 content they show two crystallization peaks (except some partially crystalline samples). T_{p1} decreases with composition faster than T_g for compositions richer in Sb_2Te_3 than the eutectic composition, indicating an enhanced crystallization tendency.

3.2. Determination of glass-forming ability from thermal data

The temperatures of structural transformations for the glassy samples are quoted in Table I. They correspond to the temperatures of the glass tran-

TABLE I Temperatures of structural transformations for glassy $(\text{GeSe}_2)_{100-y}(\text{Sb}_2\text{Te}_3)_y$ samples. Glass transition, T_g ; onset of the first crystallization peak, T_r ; and liquidus temperature T_l . Heating rate 20 K min^{-1}

y	T_g (K)	T_r (K)	T_l (K)
5	613	693	960
10	563	685	896
15	536	652	827
20	526	630	800
24	501	593	770
25	497	587	778
30	480	545	790

sition, T_g , the onset of the first crystallization peak, T_r , and the liquidus temperature, T_l . In all cases they were measured at a scan rate $\beta = 20 \text{ K min}^{-1}$, but only T_r was observed to be very sensitive to β .

One parameter usually employed to estimate the glass-forming ability is the reduced glass temperature, T_g/T_l , which, as stated by Kauzmann [16], takes a value of about $2/3$ for a large number of glassy substances [17]. Another parameter introduced by Hruby [18] is K_{gl} defined as $K_{gl} = (T_r - T_g)/(T_l - T_r)$. Regarding T_g as the temperature at which the supercooled liquid hardens to a glass, this parameter stresses the fact that the probability of obtaining a glass increases as the supercooling interval $T_l - T_g$ decreases and its stability increases with the difference $T_r - T_g$. Good glass-formers would, then, have high K_{gl} values. The reduced glass temperature and the K_{gl} parameters are plotted in Fig. 2 against composition. The present results clearly indicate that glass-forming ability exhibits a maximum near 15 to 20 mol% Sb_2Te_3 depending on the parameter considered. As K_{gl} depends on T_r and this temperature is very sensitive to β , no significant

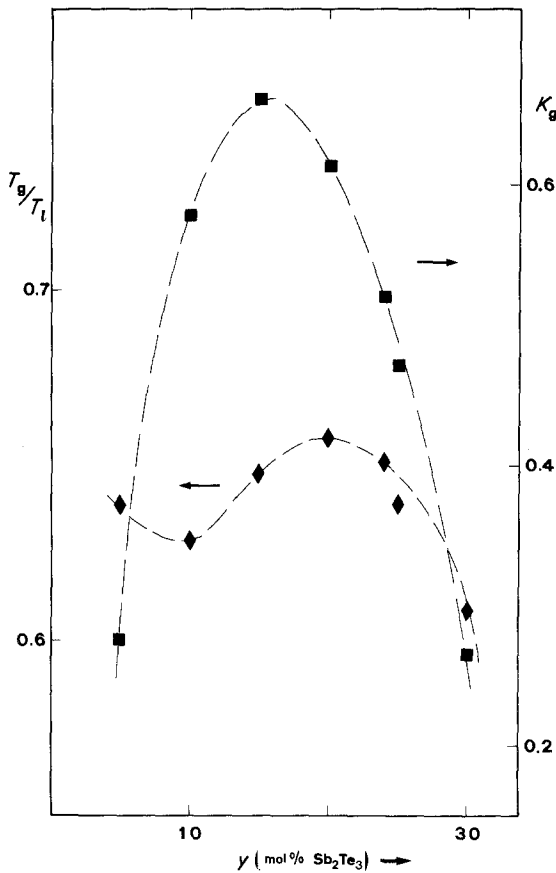


Figure 2 Glass formation parameters: T_g/T_l (\blacklozenge) and K_{gl} (\blacksquare) for the alloys investigated.

meaning can be ascribed to the differences between the two results.

3.3. Kinetics of crystallization in non-isothermal conditions

To explain the thermal behaviour on crystallization we assume that the rate of crystallization is given by

$$d\alpha/dt = k(T)f(\alpha) \quad (1)$$

Here $f(\alpha)$ is a function which depends on the mechanism of crystallization and $k(T)$ is given by the Arrhenius expression

$$k(T) = k_0 \exp(-E/RT) \quad (2)$$

where k_0 is a pre-exponential factor and E the effective activation energy. The peak method has been used to obtain the effective activation energy in non-isothermal measurements. The condition that at the peak temperature $(d^2\alpha/dt^2)_{T=T_p} = 0$ can be rewritten in terms of the constant heating rate β and the effective activation energy E as:

$$\ln(\beta E/RT_p^2) = -E/RT_p + \ln A \quad (3)$$

where A is given approximately by k_0 but depends weakly on β and the specific form of $f(\alpha)$ [10]. The activation energy E has been measured from the temperature shifts obtained on heating at scan rates ranging from 2.5 to 80 K min⁻¹. Fig. 3a

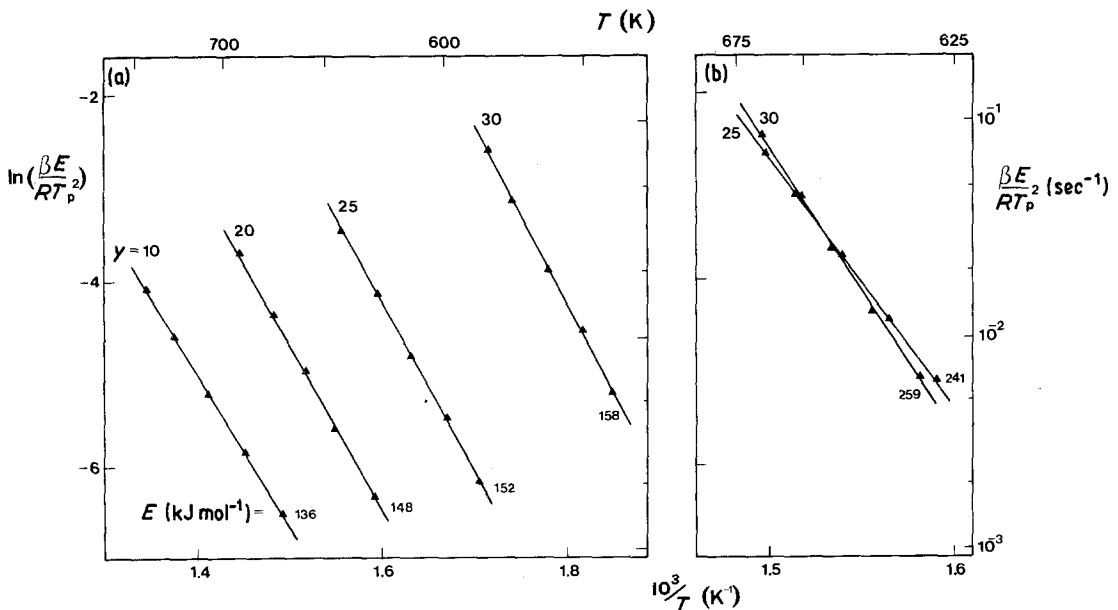


Figure 3 Plots of $\ln(\beta E/RT_p^2)$ against $1/T$ for the crystallization peaks of $(\text{GeSe}_2)_{100-y}(\text{Sb}_2\text{Te}_3)_y$ glasses. (a) First peak and (b) second peak.

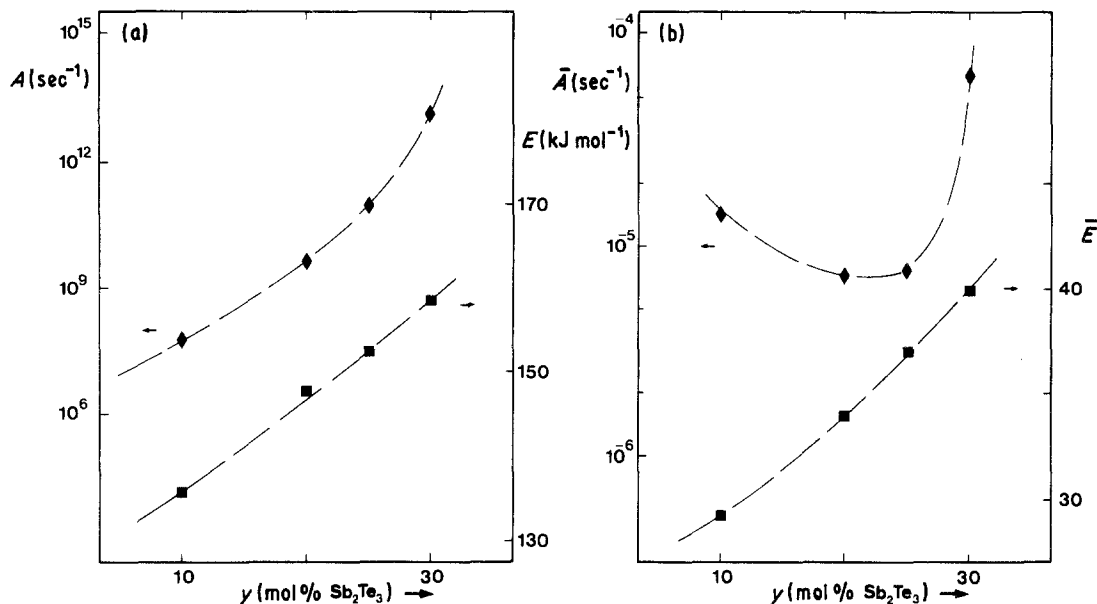


Figure 4 Composition dependence of the kinetic parameters: (a) A and E ; (b) \bar{A} and \bar{E} (as defined in Section 3.3).

shows the plots of $\ln(\beta E/RT_p^2)$ against $1/T_p$ for the first crystallization peak and Fig. 3b the same representation for the second crystallization peak. It is apparent from Fig. 3 that both E and $\ln k_0$ increase as GeSe_2 is replaced by Sb_2Te_3 . Furthermore, when a second crystallization peak is present, its effective activation energy is roughly 5/3 of that of the first crystallization peak. X-ray diffraction results on partially and totally crystallized samples suggest that the second peak is actually due to a transformation of crystalline phases already present [19], but more detailed morphological analysis is needed for a conclusion to be reached.

The effective activation energy observed on reheating a glass will be related to the glass-forming ability for the molten alloy, but the relationship is by no means obvious. One simple approach could be the use of reduced quantities. That is: reduced peak temperatures $\bar{T}_p = T_p/T_g$, reduced activation energies, $\bar{E} = E/RT_g$, as well as reduced heating rates $\bar{\beta} = \beta/T_g$. Then we can write

$$\ln(\bar{\beta}\bar{E}/\bar{T}_p^2) = \bar{E} \left(1 - \frac{1}{\bar{T}_p}\right) + \ln \bar{A} \quad (4)$$

with

$$\bar{A} \cong k_0 \exp(-\bar{E}) \quad (5)$$

The composition dependence of E , \bar{E} , A and \bar{A} is illustrated in Fig. 4. The influence of composition on the activation energy is approximately compen-

sated by that of the parameter A . As a consequence the reduced parameter \bar{A} shows a minimum near $\gamma \cong 22$ composition. It can be inferred that the resistance to crystallization is a maximum at that composition. This result reinforces those previously obtained with the parameters T_g/T_1 and K_{gl} .

3.4. Structural and morphological analysis

Optical and scanning electron microscopy were employed to observe the type and extent of crystallization obtained during the thermal treatment of the glasses. Crystallization is produced by heating bulk glasses at 20 K min^{-1} up to some pre-selected temperatures and then cooling again to room temperature [20]. These temperatures correspond to certain values of the crystallized fraction, α , or to some characteristic features of the actual DSC curve, according to the following nomenclature:

- Point A Initial stages of crystallization ($\alpha \cong 10\%$)
- Point B On the low temperature side of the first crystallization exotherm ($\alpha \cong 20\%$)
- Point C Maximum of the first crystallization peak
- Point D Final stages of crystallization

Micrographs of the partially crystallized samples exhibit typical patterns which depend critically on the composition. In the region of the primary GeSe_2 crystallization ($\gamma < 24$) the

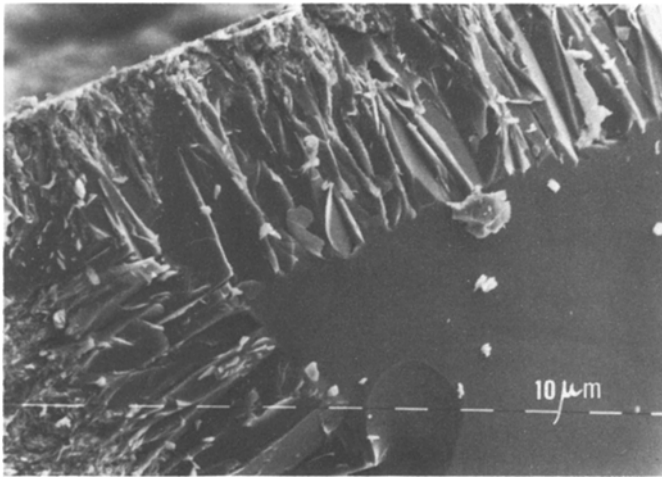


Figure 5 SEM micrograph for a $(\text{GeSe}_2)_{85}(\text{Sb}_2\text{Te}_3)_{15}$ sample showing the morphology after heating to point C.

nucleation starts preferentially from the surface, the growth front moving approximately parallel to the surface of the sample. Fig. 5 shows a SEM micrograph for a sample with $y = 15$ heated to point C. For the other compositions ($y \geq 24$) nucleation develops typically at random throughout the bulk of the sample. Optical microscopic examination of glasses heated to point A gives a surface nucleation density that increases when GeSe_2 decreases. That is, we obtain the values of $3 \times 10^8 \text{ m}^{-2}$ for $y = 24$ (eutectic composition), $1 \times 10^9 \text{ m}^{-2}$ for $y = 25$ and about 10^{10} m^{-2} for $y = 30$.

Fig. 6 shows the initial crystallites obtained by continuous heating to point B for a glass with $y = 24$. Crystalline nuclei develop in a spherulitic form. A lamellar structure is observed when crystallization is completed. The morphology of the crystals is quite different for close compositions. In Fig. 7 a series of SEM micrographs

showing the progress of crystallization on continuous heating for a sample with $y = 25$ are presented. No microstructural change can be clearly detected between the first and the second exotherm. The coalescence of crystals occurs at a smaller crystalline size as y increases. Fig. 8 shows the crystallites developed in axialitic form after heating up to point A in a sample with $y = 30$. In general, within the spatial resolution limits in energy dispersive analysis there is no concentration difference between the emerging crystallites and the vitreous matrix. Therefore eutectic crystallization is presumed for all the glasses studied. However, it was qualitatively observed by energy-dispersive analysis that water quenched partially crystalline samples ($35 \leq y \leq 50$) have the crystalline phase with a composition richer in Sb_2Te_3 than the vitreous matrix. The crystals, of lamellar morphology, correspond to the solid solution Φ , as verified by X-ray diffraction.

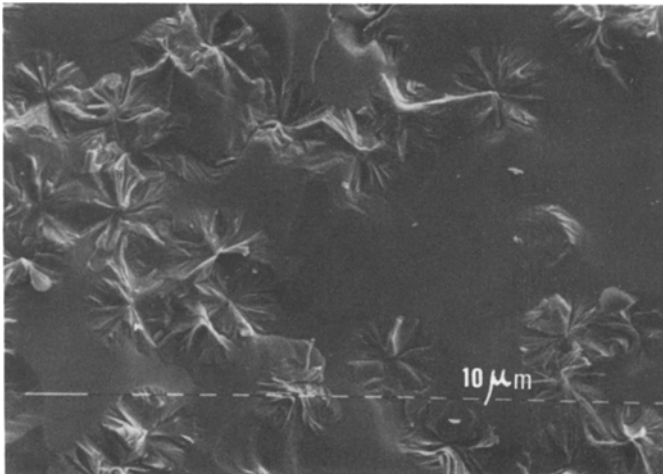


Figure 6 SEM micrograph on a fresh fracture after point B for $(\text{GeSe}_2)_{76}(\text{Sb}_2\text{Te}_3)_{24}$ alloy.

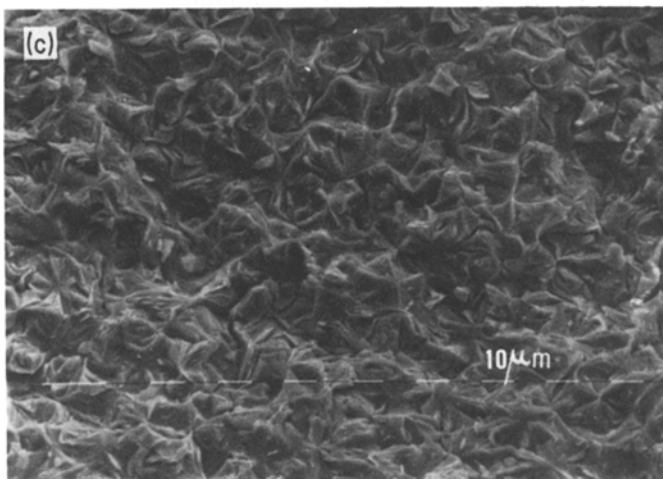
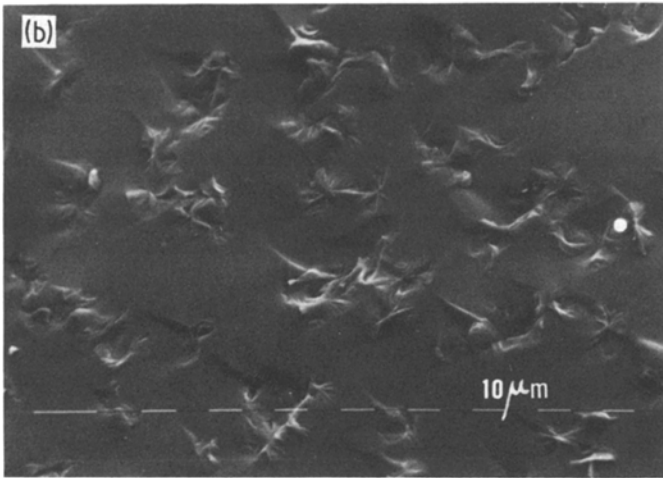
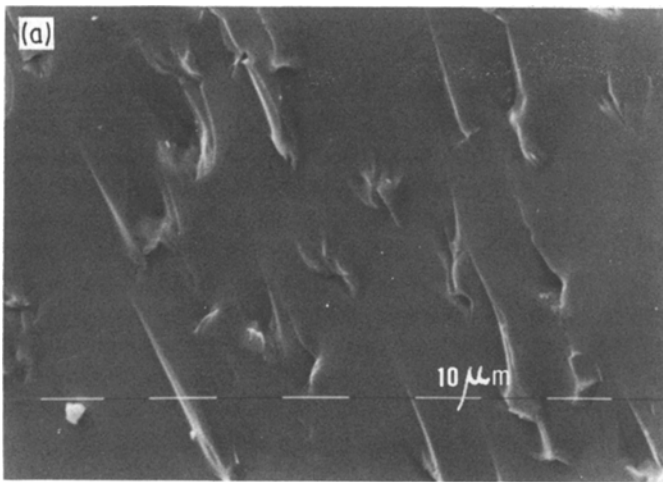


Figure 7 Progress on crystallization of $(\text{GeSe}_2)_{75}(\text{Sb}_2\text{Te}_3)_{25}$ alloy glass heated to: (a) point A; (b) point B; and (c) point D.

4. Conclusions

The formation, thermal stability and crystallization in the system $\text{GeSe}_2\text{-Sb}_2\text{Te}_3$ have been investigated by differential scanning calorimetry,

X-ray diffraction and optical and scanning electron microscopy.

The glass-forming region by water quenching extends from 5 to 30 mol% Sb_2Te_3 . Inside this

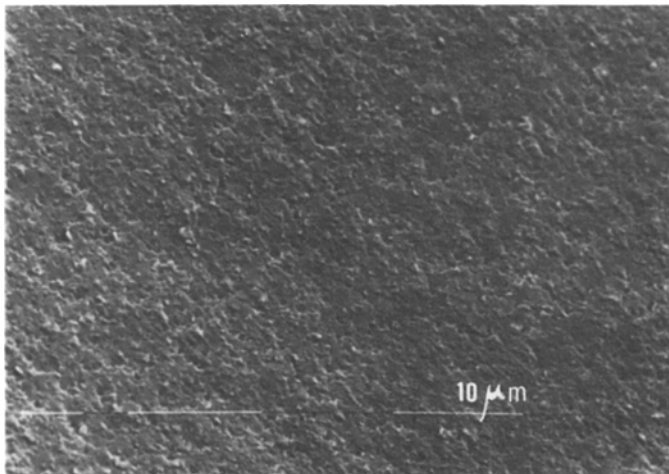


Figure 8 Axialitic structure for a $(\text{GeSe}_2)_{70}(\text{Sb}_2\text{Te}_3)_{30}$ alloy heated to point A.

domain, glass-forming ability, as measured by the reduced glass temperature T_g/T_1 and the Hruby K_g parameter, exhibits a maximum near 15 to 20 mol% Sb_2Te_3 .

Glasses in the range 5 to 20 mol% Sb_2Te_3 show a single crystallization peak on heating, but for higher Sb_2Te_3 content they show two crystallization peaks. The activation energy for each stage of crystallization has been evaluated by use of the peak method. An estimate of the pre-exponential factor k_0 has also been obtained. Both the activation energy and $\ln k_0$ increase as GeSe_2 is replaced by Sb_2Te_3 .

For compositions lying in the GeSe_2 primary crystallization region (Sb_2Te_3 content less than 24 mol%) crystals appear preferentially at the surface of the glass. For greater Sb_2Te_3 content nucleation develops typically at random in the bulk; the nucleation density, measured at fixed crystallized fractions, increases with Sb_2Te_3 content. A lamellar eutectic crystallization seems to occur in all the glasses studied.

Acknowledgements

The authors wish to thank Dr A. Alvarez for preparing the polished samples, and Ms M. Marsal for her skills in SEM and EDAX analysis. This work was supported by CAICYT, Project no. 0310/81.

References

1. D. TURNBULL, *Contemp. Phys.* **10** (1969) 473.
2. D. R. UHLMANN, *J. Non-Cryst. Solids* **7** (1972) 337.

3. P. I. K. ONORATO, D. R. UHLMANN and R. W. HOPPER, *ibid.* **41** (1980) 189.
4. J. C. PHILLIPS, *ibid.* **34** (1979) 153.
5. *Idem*, *Phys. Status Solidi (b)* **101** (1980) 473.
6. *Idem*, *J. Non-Cryst. Solids* **35/36** (1980) 1157.
7. B. T. KOLOMIETS, *Phys. Status Solidi* **7** (1964) 359, 713.
8. H. S. CHEN, *Rep. Prog. Phys.* **43** (1980) 353.
9. J. SESTAK, Proceedings of the 3rd ICTA, Vol. 2, edited by H. G. Wiedemann (Birkhäuser Verlag, Basel, 1972) p. 3.
10. D. W. HENDERSON, *J. Non-Cryst. Solids* **30** (1979) 301.
11. H. E. KISSINGER, *J. Res. Nat. Bur. Stand.* **57** (1956) 217.
12. *Idem*, *Anal. Chem.* **29** (1957) 1702.
13. U. KÖSTER, *Acta Metall.* **20** (1972) 1361.
14. U. KÖSTER and U. HEROLD, in "Topics in Applied Physics: Glassy Metals I", edited by H. J. Güntherodt and H. Beck (Springer-Verlag, Berlin, 1981) p. 225.
15. S. SURINACH, M. D. BARO and N. CLAVAGUERA, in "9ème Journée d'Etudes des Equilibres entre Phases", edited by M. T. Clavaguera-Mora (Universidad Autónoma de Barcelona, Bellaterra, 1983) p. 53.
16. W. KAUZMANN, *Chem. Rev.* **43** (1948) 219.
17. S. SAKKA and J. D. MACKENZIE, *J. Non-Cryst. Solids* **6** (1971) 145.
18. A. HRUBY, *Czech. J. Phys.* **B22** (1972) 1187.
19. M. T. CLAVAGUERA-MORA, S. SURINACH, M. D. BARO and N. CLAVAGUERA, *J. Mater. Sci.* **18** (1983) 1381.
20. S. SURINACH, Ph.D. Thesis, Universidad Autónoma de Barcelona (1983).

Received 8 August
and accepted 29 November 1983